Low-Rate Channel Coding With Complex-Valued Block Codes

Armin Dekorsy, *Associate Member, IEEE*, Volker Kuehn, *Member, IEEE*, and Karl-Dirk Kammeyer, *Member, IEEE*

***Abstract*—This paper addresses aspects of channel coding in orthogonal frequency-division multiplexing–code-division multiple access (OFDM-CDMA) uplink systems where each user occupies a bandwidth much larger than the information bit rate. This inherent bandwidth expansion allows the application of powerful low-rate codes under the constraint of low decoding costs. Three different coding strategies are considered: the combination of convolutional and repetition codes, the code-spread system consisting of one single very low-rate convolutional code and a serial concatenation of convolutional, Walsh–Hadamard and repetition code. The latter scheme is improved by combining the Walsh–Hadamard codes with an additional M-phase-shift keying modulation resulting in complex-valued Walsh–Hadamard codes (CWCs). Analytical performance evaluations will be given for these codes for the first time. The application of CWCs as inner codes in a serial code concatenation is also addressed in this paper. We derive a symbol-by-symbol maximum *a posteriori* decoding algorithm in the complex signal space in order to enable iterative decoding for the entire code. A comprehensive performance analysis by simulation of all the proposed coding schemes shows that the Walsh–Hadamard-based schemes are the best choice for low-to-medium system load. Note that even for fully loaded OFDM-CDMA systems, the concatenation with an inner complex-valued Walsh–Hadamard code leads to a bit-error rate less than 10^{-5} for an $\bar{E}_b/N_0$ of about 6 dB.**

***Index Terms*—Block codes, code-division multiple access (CDMA), concatenated coding, iterative decoding, orthogonal frequency-division multiplexing (OFDM), turbo codes.**

I. Introduction

MOBILE RADIO communication represents a rapidly growing market since the global system for mobile communications (GSM) standard has been established. Since then, third-generation mobile radio systems like the Universal Mobile Telecommunication System (UMTS) or IMT-2000 have already been standardized [1]–[4], and fourth-generation systems are currently being investigated. They will probably employ code-division multiple access (CDMA) as a multiple-access technique. An attractive alternative to the commonly used single-carrier CDMA (SC-CDMA) is multicarrier CDMA (MC-CDMA) [5]–[8]. In MC-CDMA, the entire bandwidth is divided into narrow subchannels. When orthogonal frequency-division multiplexing (OFDM) is applied, the subchannels are orthogonal and do not disturb each other. A single chip now occupies only a small fraction of the whole bandwidth and is affected by flat fading. Therefore, a one-tap equalizer suffices to eliminate channel distortion.

In this paper, we consider the uplink of an OFDM-CDMA system where the asynchronous transmissions of active subscribers prohibit the use of orthogonal scrambling codes and forces the application of pseudorandom sequences [9]. Thus, multiple-access interference (MAI) degrades overall system performance and limits system capacity. There exists primarily two possibilities to combat this degradation. On one hand, multiuser detection techniques, e.g., joint detection or interference cancellation, can be applied to eliminate multiuser interference. These methods normally incur high computational costs, especially for asynchronous transmission.

On the other hand, we can treat the interference as white Gaussian noise and improve the performance with error-correcting codes that must be powerful, especially at low signal-to-interference-plus-noise ratios (SINR). Due to the inherent spreading in CDMA systems, each user occupies a very large bandwidth, and low-rate channel coding with potentially high coding gains can be employed. In the sequel, we focus only on this latter approach with single-user detection and we do not consider multiuser detection.

A crucial question is how to perform very low-rate coding under the constraint of low computational costs. In order to illuminate the potential of channel coding and to give some concrete examples, we pursue different scenarios. First, a conventional serial concatenation of a recursive convolutional code and a repetition code is discussed. Exchanging step-by-step the code rates of both codes in favor of the convolutional code finally leads to a single very low-rate convolutional code [10], [11]. Both schemes described above can be optimally decoded by means of the Viterbi algorithm.

Instead of constructing one powerful code, it is also possible to partly replace the inner repetition code by a Walsh–Hadamard (WH) code yielding a serially concatenated coding scheme (SCCS). In this case, optimal maximum-likelihood decoding (MLD) is not applicable, but suboptimal iterative "turbo" decoding using soft-output symbol-by-symbol decoding algorithms can be implemented. The choice of WH codes can be motivated by their low decoding complexity due to the application of the fast Hadamard transformation (FHT) [6]. SCCS has already been investigated in [12]–[14] and shows promising performance improvements.

Paper approved by L. Wei, the Editor for Wireless CDMA Systems of the IEEE Communications Society. Manuscript received July 18, 2001; revised March 5, 2002 and August 25, 2002. This paper was presented in part at the 2nd International Workshop on Multicarrier Spread Spectrum, Oberpfaffenhofen, Germany, September 15–17, 1999, and in part at the 3rd International Workshop on Multicarrier Spread Spectrum, Oberpfaffenhofen, Germany, September 16–17, 2001.

A. Dekorsy is with Lucent Technologies GmbH, Bell Labs Innovations, Nuremberg D-90411, Germany (e-mail: dekorsy@lucent.com).

V. Kuehn and K.-D. Kammeyer are with the Department of Telecommunications, University of Bremen, Bremen D-28334, Germany (e-mail: kuehn@ant.uni-bremen.de; kammeyer@ant.uni-bremen.de).

Digital Object Identifier 10.1109/TCOMM.2003.811417

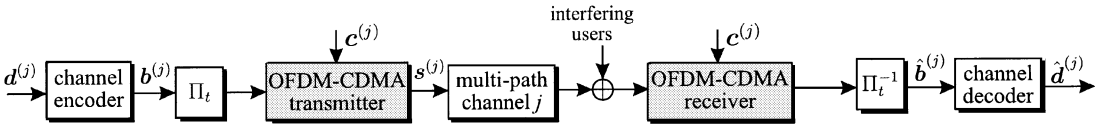

Fig. 1. Structure of OFDM-CDMA system.

This paper concentrates on an extension of WH codes by applying an additional M-phase-shift keying (PSK) modulation in order to obtain complex-valued WH block codes. The proposed combination of modulation and encoding was published for the first time as hybrid modulation in [15] where noncoherent detection was performed. The new aspect arising in this paper is the interpretation of the hybrid modulation as complex-valued block encoding. Hence, we exploit the complex signal space in context with channel coding. This offers a new kind of view, especially when a complex-valued WH code is used as the inner code in a serial concatenation.

While for the (real-valued) SCCS, iterative decoding has already been investigated [12], [14], [16], we analyze the corresponding "turbo" decoding in a complex signal space for the first time. This task requires as a first step the derivation of symbol-by-symbol maximum *a posteriori* (MAP) or Max-Log-MAP decoding for complex-valued WH codes (CWCs). Next, we optimize the complex-valued concatenation in terms of interchanging the code rates of the constituent codes. In a last step, an overall comparison of the proposed schemes concludes the investigations.

The paper consists of the following parts. Section II describes the OFDM-CDMA system consisting of transmitter, mobile radio channel, and receiver. Section III deals with the CWCs. In particular, the construction and main properties of these codes as well as maximum-likelihood, symbol-by-symbol maximum *a posteriori* (SS-MAP), and Max-Log-MAP decoding algorithms are introduced. In order to demonstrate the performance of these codes, an analytical performance derivation based on the union bound will also be presented. Section IV briefly discusses the optimization of the complex-valued SCCS and compares all considered coding schemes by simulation results. Finally, Section V concludes the paper.

II. System Description

Fig. 1 illustrates the structure of a typical OFDM-CDMA system. For simplicity, the system is only depicted for a specific user j. The remaining $J-1$ active users are summed as one interfering signal. We consider blockwise transmission with finite sequences represented as vectors, e.g., $\boldsymbol{b}^{(j)}$ consisting of symbols $b^{(j)}$.

First, the information bit vector $\boldsymbol{d}^{(j)}$ is fed into a channel encoder. As mentioned in [11], [14], and [16], spreading can be regarded as repetition coding with successive scrambling. In order to allow a clear motivation of the different coding schemes described in Section IV, the repetition encoder is incorporated into the channel encoder. Therefore, the channel encoder has a code rate that equals the reciprocal of the processing gain, $R = 1/G_P$. The duration T_b of an encoded bit then equals the final chip duration T_c, i.e., $T_b = T_c = R \cdot T_d$ where T_d is the duration of a source bit.

The interleaved version of vector $\boldsymbol{b}^{(j)}$ at the output of Π_t is fed to the OFDM-CDMA transmitter.[1] This transmitter consists of the following parts [8]. First, the symbols are scrambled with a user-specific sequence $\boldsymbol{c}^{(j)}$, $0 \le j < J$. Due to the asynchronous transmission in the uplink we use real valued pseudonoise sequences for scrambling [9]. Next, the signal is mapped onto N_M subcarriers and transformed into the time domain by the inverse fast Fourier transform (IFFT). For the remainder of the paper, N_M equals the processing gain ($G_P = N_M$). This leads to a scenario, where, on the average, one information bit is mapped onto one OFDM symbol. Finally, a guard interval (cyclic prefix) of duration T_g larger than the delay spread of the channel is inserted in front of each symbol.

The obtained signal $\boldsymbol{s}^{(j)}$ is now transmitted over a perfectly OFDM-symbol interleaved multipath Rayleigh fading channel with equal average power on each tap that remains unchanged during one OFDM symbol. Successive channel coefficients are assumed to be statistically independent.

At the receiver, the OFDM-CDMA block has to perform the following steps. After removing the guard interval, the signal is transformed into the frequency domain. Since the guard interval represents a cyclic prefix, the channel influence turns out to be a scalar multiplication of each chip with the corresponding frequency domain channel coefficient $H_\mu^{(j)}$, $\mu \in [0, N_M - 1]$ [5]. In order to apply maximum ratio combining, a simple multiplication with $\left(H_\mu^{(j)}\right)^*$ is employed [5], [14]. After subsequent detection of the real part, descrambling, and deinterleaving, the signal $\hat{\boldsymbol{b}}^{(j)}$ is fed to the channel decoder.

The SINR at the input of the channel decoder can be expressed by [14]

$$\gamma = \frac{R\frac{\bar{E}_b}{N_0}}{1 + (J-1)R\frac{\bar{E}_b}{N_0}} \tag{1}$$

with $\bar{E}_b$ as averaged energy per source bit and N_0 as noise spectral density. For unequal receive power of different users, the term $J-1$ in (1) must be replaced by $\sum_{j' \neq j} \alpha_{j'}$, where $\alpha_{j'}$ represents the power ratio between the interfering user $j' \neq j$ and the desired user j [17]. Obviously, the SINR degrades with increasing J. Therefore, strong error-correcting codes operating at low SINR have to be employed in systems with high load and single-user detection.

III. Complex-Valued WH Codes

In this section, we present WH codes extended by an additional M-PSK modulation in order to obtain complex-valued

[1]This interleaving avoids burst errors and is required independent of the coding scheme applied. The interleaver length is determined by the delay constraints of the transmission.

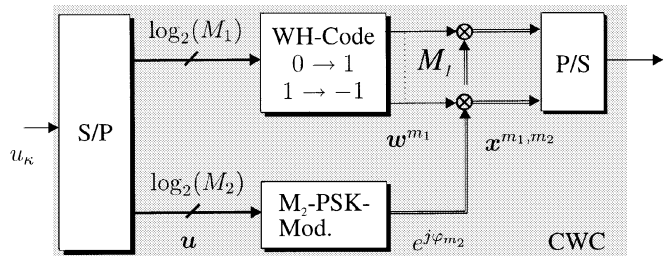

Fig. 2. Construction of a CWC.

WH block codes (CWCs). The proposed combination of modulation and encoding was presented as hybrid modulation in [15]. The new aspect arising in this paper is the interpretation of the hybrid modulation as complex-valued block encoding. This view presents new, fundamental aspects that were partly published in [16] and [18]. Here, we introduce the SS-MAP decoding rule that is required when a CWC is employed in a SCCS. Furthermore, we give an analytical derivation of the performance that is based on the well-known union bound for a fully interleaved flat Rayleigh fading channel. We note that the proposed combination of modulation and encoding need not be restricted to WH codes. Generalized complex-valued codes might be an interesting task for future analysis.

A. Construction and Properties

Fig. 2 illustrates the construction of CWCs. A block of $(\log_2(M_1)+\log_2(M_2))$ data bits $u_\kappa \in \{0,1\}$, each of duration T_d, is serial-parallel converted into an information word $\boldsymbol{u}$. Then, $\boldsymbol{u}$ is divided into components of $\log_2(M_1)$ and $\log_2(M_2)$ data bits, respectively.

The first part is fed to the $(M_1, \log_2(M_1), M_1/2)$-WH encoder that maps $\log_2(M_1)$ bits onto a WH code word $\boldsymbol{w}^{m_1} = [w_0^{m_1}, w_1^{m_1}, \ldots, w_{M_1-1}^{m_1}]^T$ with $m_1 \in \{0, M_1-1\}$. This mapping includes the conversion ($0 \to 1$ and $1 \to -1$) and is well known as M_1-ary Walsh modulation [8], [16]. The received word consists of Walsh chips $w_\mu^{m_1}$, $\mu \in [0, M_1-1]$.

In the lower branch of Fig. 2, the remaining $\log_2(M_2)$ data bits are mapped onto a PSK symbol $e^{j\varphi_{m_2}}$, $m_2 \in \{0, \ldots, M_2-1\}$. We will show later that the error-correction capability of the proposed code primarily depends on the phase differences of the applied M_2-PSK modulation scheme. Rotation of the signal constellation has no impact. In order to have a clear distinction between the two parts of $\boldsymbol{u}$, the first $\log_2(M_1)$ bits are termed Walsh bits, whereas the $\log_2(M_2)$ bits of the second part are called modulation phase bits.

Complex block coding is accomplished by multiplying the WH code word $\boldsymbol{w}^{m_1}$ with the modulation symbol $e^{j\varphi_{m_2}}$. Notice that each Walsh chip is multiplied with the same modulation symbol. The resulting complex-valued code word is, therefore, given by $\boldsymbol{x}^{m_1,m_2} = \boldsymbol{w}^{m_1} e^{j\varphi_{m_2}}$ with code symbols $x_\mu^{m_1,m_2} = w_\mu^{m_1} e^{j\varphi_{m_2}}$.

Obviously, we obtain simple WH codes for $M_2 = 1$. With $M_2 = 2$, the described construction leads to Reed–Muller codes [19]. The choice of $M_2 \geq 4$ yields complex-valued block codes. Furthermore, the encoder is nonsystematic except for $M_2 = 1$. In order to simplify notation, we can denote the code words by $\boldsymbol{x}^i = \boldsymbol{w}(\boldsymbol{x}^i)e^{j\varphi(\boldsymbol{x}^i)}$, where subscript i indicates the ith word with $i \in \{0, \ldots, M_1 \cdot M_2 - 1\}$. In this sense, $\boldsymbol{w}(\boldsymbol{x}^i)$ denotes the WH code word, and $\varphi(\boldsymbol{x}^i)$ the M_2-PSK phase of code word $\boldsymbol{x}^i$, respectively.

TABLE I
SINR GAIN $\Delta\gamma$ AT THE DECODER INPUT FOR QPSK ($M_2 = 4$) AND $M_1 = 4$ TO $M_1 = 256$

M_1	4	8	16	32	64	128	256
$\Delta\gamma$ in dB	3.00	2.20	1.76	1.46	1.25	1.09	0.97

The proposed combination of WH encoding and PSK modulation yields a complex-valued code consisting of $M_1 \cdot M_2$ code words. It has the code rate

$$R_{\mathrm{CWC}} = \frac{\log_2(M_1 \cdot M_2)}{M_1} = R_{\mathrm{WH}} + \frac{\log_2(M_2)}{M_1} \tag{2}$$

where $R_{\mathrm{WH}} = \log_2(M_1)/M_1$ denotes the rate of the inherent WH code. Hence, CWCs have a higher code rate for $M_2 \geq 2$ than simple WH codes of the same code-word length M_1. Assuming a fixed source data rate, the extension of WH codes by the proposed phase modulation leads to a bandwidth reduction by factor $\log_2(M_1 \cdot M_2)/\log_2(M_1)$. Otherwise, the data rate can be increased by this factor if the entire bandwidth remains constant.

Moreover, for a fixed energy E_b per source bit, the energy per code symbol is given by $E_c = E_b \cdot R_{\mathrm{CWC}}$. Since the energy per code symbol equals the signal energy at the decoder input (provided that matched filtering at chip rate is applied), the SINR at the decoder input increases with growing code rate. The SINR gain can be expressed in decibels by

$$\Delta\gamma = 10\log_{10}\left(\frac{\mathrm{SINR}_{\mathrm{CWC}}}{\mathrm{SINR}_{\mathrm{WH}}}\right) = 10\log_{10}\left(\frac{R_{\mathrm{CWC}}}{R_{\mathrm{WH}}}\right). \tag{3}$$

Table I lists $\Delta\gamma$ for $M_2 = 4$ quaternary phase-shift keying (QPSK) and different values of M_1.

The distance spectrum is another significant property of coding schemes. Due to the complex-valued code words, Euclidian distance has to be taken into account rather than the Hamming distance as in the case of binary encoding. Therefore, the analysis in terms of error-correction capability should be performed in Euclidean space.

Generally, the squared Euclidean distance between two code words $\boldsymbol{x}^i$, $\boldsymbol{x}^j$ of a complex-valued block code of length M_1 can be expressed by

$$\begin{aligned} e_W^2(i,j) &= \sum_{\mu=0}^{M_1-1} \varepsilon_\mu^2(i,j) \\ &= 2M_1 - 2\cos\left(\varphi(\boldsymbol{x}^i) - \varphi(\boldsymbol{x}^j)\right) \\ &\quad \times \sum_{\mu=0}^{M_1-1} w_\mu(\boldsymbol{x}^i) w_\mu(\boldsymbol{x}^j) \end{aligned} \tag{4}$$

where

$$\varepsilon_\mu^2(i,j) = \left|x_\mu^i - x_\mu^j\right|^2 \tag{5}$$

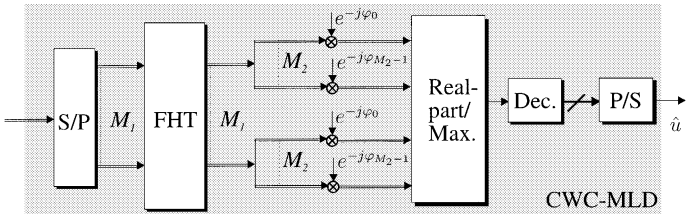

Fig. 3. MLD of complex-valued code words.

describes the distance between two code symbols x_μ^i, x_μ^j at position μ of the considered pair of code words. Equation (4) shows that the chosen M_2-PSK modulation determines the distance between two code words as the cosine of the phase difference between two points of the underlying signal constellation. Rotation of the signal constellation has no impact on the distance.

By increasing M_2, we reduce the squared Euclidian distance, but, otherwise, the code rate is increased according to (2). An analysis of this tradeoff in [20] shows that QPSK modulation is best suited. Therefore, we will confine our discussion to QPSK ($M_2 = 4$, $\Delta\varphi = (\varphi(\boldsymbol{x}^i) - \varphi(\boldsymbol{x}^j)) \in \{0, \pm\pi/2, \pi\}$) throughout the paper. For QPSK, (4) reduces to

$$e_W^2(i,j) = \begin{cases} 4M_1, & \boldsymbol{w}(\boldsymbol{x}^i) = \boldsymbol{w}(\boldsymbol{x}^j) \wedge \Delta\varphi = \pi \\ 2M_1, & \text{else} \end{cases} \tag{6}$$

and the squared Euclidean distance between two code symbols can be expressed by

$$\varepsilon_\mu^2(i,j) = \left|x_\mu^i - x_\mu^j\right|^2 = \begin{cases} 0, & w_\mu(\boldsymbol{x}^i) = w_\mu(\boldsymbol{x}^j) \wedge \Delta\varphi = 0 \\ 2, & w_\mu(\boldsymbol{x}^i) = -w_\mu(\boldsymbol{x}^j) \wedge \Delta\varphi = \pi \\ & \Delta\varphi = \pm\frac{\pi}{2} \\ 4, & w_\mu(\boldsymbol{x}^i) = w_\mu(\boldsymbol{x}^j) \wedge \Delta\varphi = \pi \\ & w_\mu(\boldsymbol{x}^i) = -w_\mu(\boldsymbol{x}^j) \wedge \Delta\varphi = 0 \end{cases}. \tag{7}$$

Equation (6) shows that there exists only one code word with a code word distance of $4M_1$. This complex-valued code word comprises the same WH word $\boldsymbol{w}(\boldsymbol{x}^0) = \boldsymbol{w}(\boldsymbol{x}^j)$, but its QPSK symbol is antipodal to that of the reference (zero) word. In Section III-C, we treat this specific code word separately.

In summary, the suggested combination of WH codes with QPSK modulation benefits from a higher code rate (2), and, hence, from an improved spectral efficiency. Note that this advantage is gained without loss of error-correction capability. According to (6), all pairs of code words except one have the same distance $2M_1$ as conventional WH codes [21].

B. MLD and SS-MAP Decoding

Fig. 3 shows the code-word specific MLD of QPSK-based CWCs. MLD can be performed by the FHT followed by a multiplication with all possible complex conjugated QPSK symbols. Remember that encoding is done by multiplying a complete WH code word with one QPSK symbol. Hence, it is possible to interchange the FHT and QPSK detection in the receiver. Nevertheless, the conventional FHT can still be applied, although its input is now complex valued. Finally, a maximum decision of the real parts and a demapping of the decided code word onto $\log_2(M_1 M_2)$ data bits has to be applied.

With regard to the application of the CWC as an inner code in a serial code concatenation, we will briefly derive the SS-MAP decoding. Since this paper deals with OFDM, we assume transmission over a memoryless channel. This leads to the received vector $\boldsymbol{y} = [y_0, \ldots, y_{M_1-1}]^T$ at the decoder input with components

$$y_\mu = x_\mu^i H_\mu + n_\mu, \qquad \mu \in [0, M_1 - 1] \tag{8}$$

where x_μ^i represents the transmitted code symbol, n_μ the additive white Gaussian noise (AWGN) including multiuser interference, and H_μ the corresponding channel coefficient in the frequency domain. The noise variance $\sigma_n^2 = \gamma^{-1}$ is determined by (1). With these assumptions, we can express the log-likelihood ratio (LLR) at the output of the decoder by [22]

$$L(\hat{u}_\kappa) = \ln \frac{\sum_{\boldsymbol{x}^i \in \mathcal{X}_\kappa^1} \prod_{\mu=0}^{M_1-1} f\left(y_\mu | x_\mu^i\right) P(\boldsymbol{x}^i)}{\sum_{\boldsymbol{x}^i \in \mathcal{X}_\kappa^{-1}} \prod_{\mu=0}^{M_1-1} f\left(y_\mu | x_\mu^i\right) P(\boldsymbol{x}^i)}. \tag{9}$$

In (9), $\mathcal{X}_\kappa^{\pm 1}$ describes the set of complex-valued code words $\boldsymbol{x}^i$, $i \in [0, M_1 M_2 - 1]$, with information bit $u_\kappa = \pm 1$ at time instance κ.[2] Moreover, $P(\boldsymbol{x}^i)$ is the *a priori* probability (APP) of code word $\boldsymbol{x}^i$. The probability density function $f(y_\mu | x_\mu^i)$ is given by

$$\begin{aligned} f\left(y_\mu | x_\mu^i\right) &= \frac{1}{\pi\sigma_n^2} \cdot \exp\left\{-\frac{\left|y_\mu - x_\mu^i H_\mu\right|^2}{\sigma_n^2}\right\} \\ &= \frac{1}{\pi\sigma_n^2} \cdot \exp\left\{-\frac{|y_\mu|^2 + |H_\mu|^2}{\sigma_n^2}\right\} \\ &\quad \cdot \exp\left\{\frac{2\,\Re\left\{y_\mu \cdot \left(x_\mu^i\right)^* H_\mu^*\right\}}{\sigma_n^2}\right\} \end{aligned} \tag{10}$$

since $\left|x_\mu^i\right|^2 = 1$ holds. In order to simplify notation, we introduce the parameter $L_\mu = (2/\sigma_n^2) H_\mu^* y_\mu$. Inserting L_μ and (10) in (9) leads to

$$L(\hat{u}_\kappa) = \ln \frac{\sum_{\boldsymbol{x}^i \in \mathcal{X}_\kappa^1} \exp\left\{\Re\left\{\sum_{\mu=0}^{M_1-1} L_\mu \cdot \left(x_\mu^i\right)^*\right\}\right\} P(\boldsymbol{x}^i)}{\sum_{\boldsymbol{x}^i \in \mathcal{X}_\kappa^{-1}} \exp\left\{\Re\left\{\sum_{\mu=0}^{M_1-1} L_\mu \cdot \left(x_\mu^i\right)^*\right\}\right\} P(\boldsymbol{x}^i)}. \tag{11}$$

It is now remarkable that the inner sum of (11) can be computed by the formerly introduced FHT with phase detection. The input values are the L-values L_μ. Furthermore, the APP of a code word can be expressed by

$$\begin{aligned} P(\boldsymbol{x}^i) &= \prod_{\kappa=0}^{\log_2(M_1 \cdot M_2)-1} P(u_\kappa = \pm 1) \\ &= \prod_{\kappa=0}^{\log_2(M_1 \cdot M_2)-1} \frac{e^{\frac{1}{2}L(u_\kappa)}}{1 + e^{L(u_\kappa)}} e^{\frac{1}{2}L(u_\kappa)u_\kappa} \end{aligned} \tag{12}$$

where $L(u_\kappa)$ indicates the *a priori* LLR of information bit u_κ. Finally, (12) is inserted in (11) and the SS-MAP decoding rule for the information bits of the complex-valued codes is obtained as shown in (13) at the bottom of the next page.

Because of high computational costs as well as problems with fixed-point representation of huge LLR values, we have

[2]It is assumed that a logical zero is mapped onto $u_\kappa = 1$ and a logical one onto $u_\kappa = -1$.

applied the suboptimum Max-Log-MAP decoder [22]. Exploiting the approximation $\log_2(\sum_\chi e^{x_\chi}) \approx \max_\chi\{x_\chi\}$, the Max-Log-MAP decoding rule can be expressed as

$$L(\hat{u}_\kappa) \approx \max_{\boldsymbol{x}^i \in \mathcal{X}_\kappa^1} \left\{ \Re\left\{ \sum_{\mu=0}^{M_1-1} L_\mu \cdot \left(x_\mu^i\right)^* \right\} + \sum_{\lambda=0}^{\log_2(M_1\cdot M_2)-1} \frac{1}{2} L(u_\lambda) u_\lambda \right\} - \max_{\boldsymbol{x}^i \in \mathcal{X}_\kappa^{-1}} \left\{ \Re\left\{ \sum_{\mu=0}^{M_1-1} L_\mu \cdot \left(x_\mu^i\right)^* \right\} + \sum_{\lambda=0}^{\log_2(M_1\cdot M_2)-1} \frac{1}{2} L(u_\lambda) u_\lambda \right\}. \quad (14)$$

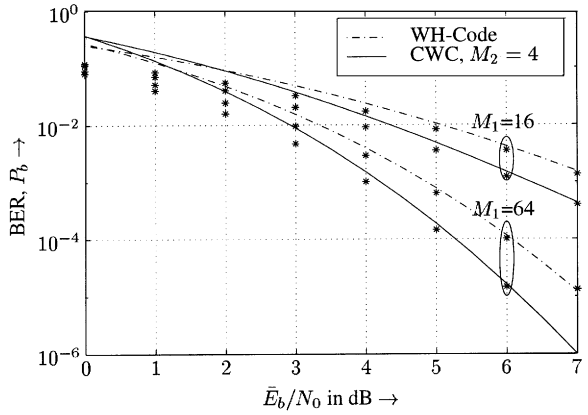

Fig. 4. Union bound of CWC with rates $R_{\mathrm{CWC}} = 6/16$ and $R_{\mathrm{CWC}} = 8/64$ for a perfectly interleaved one-path Rayleigh fading channel. WH codes with rates $R_{\mathrm{WH}} = 4/16$ and $R_{\mathrm{WH}} = 6/64$ are also shown. Simulation results: $*$.

C. Performance Analysis

Due to our focus on OFDM-CDMA systems, we will briefly derive the bit-error probability P_b by using the well-known union bound for a fully interleaved one-path Rayleigh fading channel. We assume perfect channel state information, equalization with the complex conjugate channel coefficient, and a nondissipative channel. Since the distances given in (6) are independent of the chosen reference word, $\boldsymbol{x}^0 = [1, \ldots, 1]$ can be used as a reference. A received code symbol at the decoder input is, therefore, given by $y_\mu = |H_\mu|^2 x_\mu^0 + H_\mu^* n_\mu$. Again, $|H_\mu|^2$ is chi-squared distributed and n_μ represents AWGN including multiuser interference.

Let us start with the code-word specific pairwise error probability denoted by P_2 [23]. First, we define $D(0,j)$ as the effective length of error events, i.e., the code word $\boldsymbol{x}^j$ differs in $D(0,j)$ positions from the reference word $\boldsymbol{x}^0$. Note that for CWCs, the code symbol distances $\varepsilon_\mu^2(0,j)$ in (7) are identical at these $D(0,j)$ positions. Hence, we can omit the subindex μ. With (4) and (6) this yields

$$e_W^2(0,j) = D(0,j) \cdot \varepsilon^2(0,j) = \begin{cases} 4\,M_1, & \boldsymbol{w}(\boldsymbol{x}^0) = \boldsymbol{w}(\boldsymbol{x}^j) \wedge \Delta\varphi = \pi \\ 2\,M_1, & \text{else.} \end{cases} \quad (15)$$

As mentioned before, there exists only one code word with code-word distance $4M_1$.

With these assumptions the code-word specific pairwise error probability can be expressed by

$$P_2\left(\varepsilon^2(0,j), D(0,j)\right) = \left(\frac{1-\nu}{2}\right)^{D(0,j)} \times \sum_{l=0}^{D(0,j)-1} \binom{D(0,j)-1+l}{l} \times \left(\frac{1+\nu}{2}\right)^{l} \quad (16)$$

with

$$\nu = \sqrt{\frac{\bar{\gamma}_e}{1+\bar{\gamma}_e}}$$

and

$$\bar{\gamma}_e = \frac{1}{4}\varepsilon^2(0,j)\gamma. \quad (17)$$

Parameter γ is given by(1). A detailed derivation of the code-word specific pairwise error probability can be found in [21]. With (16) and (17) it becomes obvious that the code symbol distance $\varepsilon^2(0,j)$ affects the SINR, whereas the effective length of error events $D(0,j)$ determines the diversity degree of the coding scheme.

Using the pairwise error probability given in (16), the union bound on the bit-error rate (BER) of a fully interleaved one-path Rayleigh fading channel can be expressed by [21]

$$P_b \le \left[\sum_w \frac{w}{K} \sum_{\varepsilon^2 \in [2,4]} A_{w,\varepsilon^2} P_2\left(\varepsilon^2, \frac{2\,M_1}{\varepsilon^2}\right) \right] + \frac{2}{K} P_2(4, M_1) \quad (18)$$

where $K = \log_2(M_1 \cdot 4)$ denotes the length of an information word. Here, we count all code words with identical input weight w as well as identical code symbol distance $\varepsilon^2(0,j)$. This yields a modified form of the well-known input–output weight enumerating function (IOWEF) [23] as shown in (19) at the bottom of the next page. In (19), A_{w,ε^2} denotes the number of code words with input weight w and code symbol distance ε^2. The term at the end of (18) belongs to the code word with code-word distance $4M_1$ that is separately treated.

$$L(\hat{u}_\kappa) = \ln \frac{\sum_{\boldsymbol{x}^i \in \mathcal{X}_\kappa^1} \exp\left\{ \Re\left\{ \sum_{\mu=0}^{M_1-1} L_\mu \cdot \left(x_\mu^i\right)^* \right\} + \sum_{\lambda=0}^{\log_2(M_1\cdot M_2)-1} \frac{1}{2} L(u_\lambda) u_\lambda \right\}}{\sum_{\boldsymbol{x}^i \in \mathcal{X}_\kappa^{-1}} \exp\left\{ \Re\left\{ \sum_{\mu=0}^{M_1-1} L_\mu \cdot \left(x_\mu^i\right)^* \right\} + \sum_{\lambda=0}^{\log_2(M_1\cdot M_2)-1} \frac{1}{2} L(u_\lambda) u_\lambda \right\}} \quad (13)$$

Verification of the derived upper bound is accomplished by comparing it with Monte–Carlo simulation results in Fig. 4. The chosen parameters for the used complex-valued codes are $M_1 = 16$ and $M_1 = 64$, both with a fixed QPSK modulation ($M_2 = 4$). Hence, their code rates are $R_{\mathrm{CWC}} = 6/16$ and $R_{\mathrm{CWC}} = 8/64$, respectively. Both codes are compared to (real-valued) WH codes of the same code word length and corresponding rates $R_{\mathrm{WH}} = 4/16$ and $R_{\mathrm{WH}} = 6/64$.

First, Fig. 4 illustrates the convergence of the union bound for BERs below 10^{-3}, confirming the correctness of our derivation. A comparison of CWCs with their real-valued counterparts indicates significantly better performance for the CWC. We already worked out in Section III-A that the extension by QPSK provides the decoder with a better SINR due to the increased code rate. Besides this advantage, there exists a nearly identical distance spectrum, and, hence, the same error-correction capability. The combination of these effects results in lower BERs. For example, we observe a gain in $\bar{E}_b/N_0$ of about 0.8 dB at a BER of 10^{-3} in the case of $M_1 = 64$. Therefore, these results illustrate the advantage of exploiting the complex signal space in conjunction with WH coding.

IV. Comparison of Different Coding Schemes

A. Introduction of Coding Schemes

One characteristic feature of CDMA is the inherent bandwidth expansion, resulting in a certain robustness against multipath propagation. Conventionally, spreading by a factor N_p is simply carried out by repeating each bit N_p times, which can be interpreted as repetition coding [10], [11], [14] and successive scrambling with a user-specific sequence. Therefore, if the repetition is counted as part of the channel coding of a communication system, only the scrambling remains a CDMA-specific task. Hence, the system part between channel encoder and decoder depicted in Fig. 1 can be regarded as a user-specific time-discrete super channel.

In this paper, we distinguish three different coding scenarios. In order to ensure the same processing gain G_P for all systems, the different coding schemes have the same overall code rate

$$R = \frac{1}{N_M} = \frac{1}{G_P} = \frac{1}{64}. \tag{20}$$

This leads to a scenario, where, on average, one information bit is mapped onto one OFDM symbol.

Conventional Coding Scenario: The conventional coding system employs a convolutional code of constraint length $L_c = 7$, code rate $R_{\mathrm{CC}} = 1/n$, and generator polynomials (133_8, 171_8). Successive repetition encoding with rate

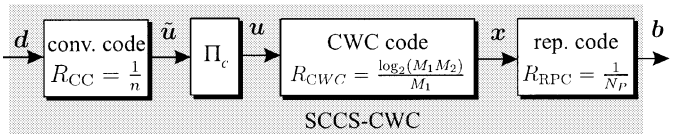

Fig. 5. Complex-valued SCCS-CWC.

$R_{\mathrm{RPC}} = 1/N_P = n/G_P$ ensures a constant overall code rate $R = R_{\mathrm{CC}} \cdot R_{\mathrm{RPC}} = 1/G_P$. To illustrate the influence of choosing R_{CC} and R_{RPC}, two combinations have been examined in our investigations. The decoder consists of a combiner that correlates N_P successive samples[3] (decoding the repetition code) followed by a Viterbi decoder.

Code-Spread System: It is well known that repetition codes have very poor error-correcting capabilities. Thus, the question arises as to whether they can be replaced by a more powerful code. Reducing R_{CC} to the minimum value of $R = 1/G_P$ results in a single very low-rate convolutional code and the repetition code is discarded. Many ideas of so-called code spreading are encapsulated in [10]. In [24], an enormous number of low-rate convolutional codes found by computer search are listed. These codes have a maximum free distance d_f and a minimum number of sequences with weight d_f. The advantage of the code-spread system employing only one very low-rate code over concatenated coding schemes (except concatenation with a repetition code) is the possibility of optimal MLD by the Viterbi algorithm. However, the obtained codes also include a kind of unequal repetition code, i.e., different symbols of a code word are repeated unequally [24].

SCCS: Replacing the inner repetition code by a more powerful code, e.g., a conventional WH code [14] or a complex-valued CWC, leads to a SCCS consisting of a convolutional code, a WH code or CWC, and a repetition code of higher rate. For the following description, we restrict attention to a CWC as depicted in Fig. 5. Although recursive convolutional codes are often used as inner codes in SCCSs [25], we prefer WH codes because of their low decoding costs (FHT).

In this paper, the code rate of the convolutional code was fixed at $R_{\mathrm{CC}} = 1/2$. Hence, introducing the CWC affects only the repetition code whose code rate R_{RPC} increases in the same way as R_{CWC} decreases (see Table II). Simulation results have shown that lower rates of the outer convolutional code (e.g., $R_{\mathrm{CC}} = 1/6$) coming along with higher rates of the inner codes (e.g., $R_{\mathrm{RPC}} = 1$) lead to a significant performance loss [14]. This observation indicates that it is important to increase the performance of the inner codes, i.e., the CWC. The interleaver Π_c

[3]Due to the one-tap equalization described in Section II, maximum ratio combining is performed.

$$A_{w,\varepsilon^2} = \begin{cases} 1 & w = 0 \wedge \varepsilon^2 = 0 \\ \binom{\log_2(M_1)}{w-1} \cdot 2 & w \in [1, \log_2(M_1) + 1] \wedge \varepsilon^2 = 2 \\ \binom{\log_2(M_1 \cdot 4)}{w} - A_{w,2} & w \in [1, \log_2(M_1\ 4)] \setminus \{2\} \wedge \varepsilon^2 = 4 \\ \binom{\log_2(M_1 \cdot 4)}{2} - A_{2,2} - 1 & w = 2 \wedge \varepsilon^2 = 4 \\ 0 & \text{else} \end{cases} \tag{19}$$

TABLE II
MAIN PARAMETERS OF SCCS WITH $M_1 = 16$

$R \stackrel{!}{=} 1/64$

No.	R_{CC}	R_{WH}, R_{CWC}	R_{RPC}	L_Π
1	1/2	4/16	1/8	600
2	1/2	6/16	1/12	600
3	1/3	6/16	1/8	900

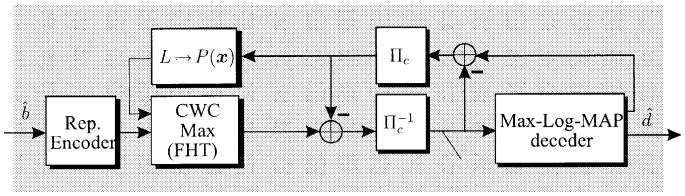

Fig. 6. Iterative decoding of complex-valued SCCS-CWC.

between convolutional and CWC encoder is a randomly chosen interleaver of length $N = 600$ or $N = 6000$[4].

Decoding of the SCCS-CWC scheme can be performed efficiently by a recursive structure as depicted in Fig. 6. First, the repetition code is decoded by means of correlation. Then, an iterative decoding process starts, consisting of an inner symbol-by-symbol Max-Log-MAP decoder for the CWC and an outer symbol-by-symbol Max-Log-MAP decoder for the convolutional code. The extrinsic information of each decoder is extracted and fed to the successive decoder. This "turbo decoding" improves the performance significantly when compared with a single decoding iteration.

Simulation Environment: The following subsections present results obtained by Monte–Carlo simulations. Since mobile radio channels are generally frequency selective for wideband CDMA transmission, we have chosen a four-path Rayleigh fading channel model. Detailed simulations show that the specific number of paths as well as the power distribution among these paths have only a minor impact on the relative performance of different coding schemes. Results with a different number of path channels are not shown in the paper due to the restricted paper length. Moreover, perfect OFDM symbol interleaving is assumed (see Section II), i.e., the interleaving depth of Π_t is much larger than the coherence time of the channel.

In a first step, we discuss the optimization of the SCCS with special focus on the complex-valued SCCS-CWC. Next, a comprehensive comparison with the competitive coding schemes is drawn. For all the simulations considered, we assumed perfect synchronization as well as perfect knowledge of the channel. Moreover, due to the mapping of one information bit to one OFDM symbol[5] and an entire code rate of $R = 1/64$, the number of carriers equals $N_M = 64$. Finally, Max-Log-MAP decoding is always applied for the block as well as convolutional code in case of serial concatenation.

B. Optimization of SCCS-CWC

A detailed optimization of the SCCS including the constituent codes and the interleaver can be found in [13] and [14]. Starting with the optimization of the outer convolutional code, it turns out that codes with low memory achieve better performance than codes with high memory [14]. It is important to note that low-memory codes have the additional advantage of low decoding complexity, which is of particular importance in the context of iterative decoding. The SCCS with an outer code of large constraint length only performs better asymptotically (for high SINR). In [21], a detailed analysis of optimizing the constraint length in connection with the complex-valued coding scheme yields the same conclusions. Based on these results, the constraint length is chosen to be $L_c = 3$ for the following examination.

In this paper, we are especially interested in exchanging the code rates for the constituent codes under the constraint of an unchanged overall code rate of the whole scheme. For example, by replacing the WH code with its complex-valued counterpart, it is possible to choose a more powerful repetition code or an outer convolutional with lower code rate. Table II summarizes some possible parameter sets for the complex-valued schemes considered here.

Moreover, all systems consist of an inner block code with code-word length $M_1 = 16$. While system (1) uses WH encoding with $R_{\mathrm{WH}} = 4/16$, complex-valued block encoding with $R_{\mathrm{CWC}} = 6/16$ is applied in system (2) as well as in (3). When replacing the WH code in system (1) with the corresponding complex-valued code in system (2), the gain in bandwidth is spent on a more powerful inner repetition code. Contrarily, we strengthen the outer convolutional code in system (3). Under the constraint of a constant interleaving delay for all scenarios, the interleaver length L_Π in system (3) becomes larger due to the lower code rate of the convolutional code.

Fig. 7 shows the BER achieved by Monte–Carlo simulations for the three different coding schemes of Table II. Only one single user is active ($J = 1$) and iterative decoding is applied for $I = 1$ as well as $I = 10$ iterations. First, the results indicate that system (2) with the more powerful complex-valued block code outperforms the other schemes for $\bar{E}_b/N_0$ larger than approximately 2 dB. This result is independent of the number of iterations and confirms the well-known fact that it is beneficial to strengthen the inner code of serially concatenated schemes [14], [26]. For $I = 10$ iterations, we observe that the curve of system (1) flattens out, whereas the complex-valued systems (2) and (3) still show a steep descent. Responsible for the sustained descent is a higher *average*[6] minimum distance of the complex-based schemes. Remember that the complex block code and the WH code have nearly identical distance properties. However,

[4]The shorter interleaver may be suited for full duplex speech transmission, whereas the longer one is restricted to data transmission with weaker delay constraints.

[5]For the SCCS as well as SCCS-CWC, we map one bit to one symbol in the average.

[6]In terms of average due to the random interleaver applied here.

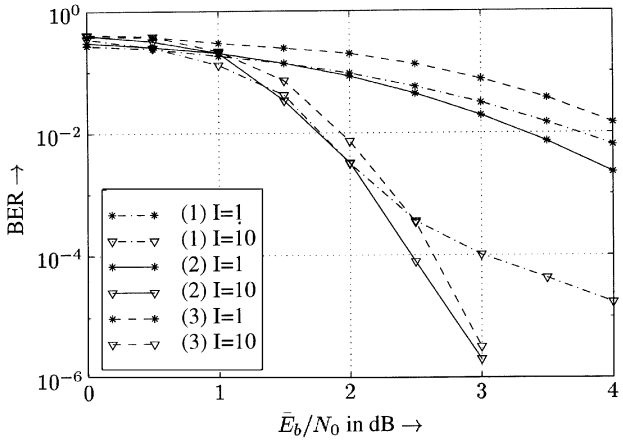

Fig. 7. Exchange of code rates for the SCCS-CWC with $M_1 = 16$, $J = 1$ users, and $I = 1$ as well as $I = 10$ iterations.

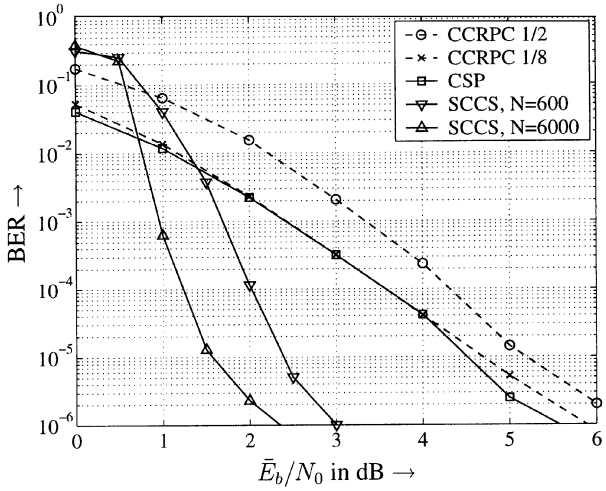

Fig. 8. Comparison of different coding schemes for $J = 1$ users, and $I = 10$ iterations for the SCCS.

TABLE III
MAIN PARAMETERS OF CODING SCHEMES

$R \stackrel{!}{=} 1/64$

No.		L_c	R_{cc}	R_{WH}, R_{CWC}	R_{RPC}
1	CCRPC	7	1/2	-	1/32
2		7	1/8	-	1/8
3	CSP	7	1/64	-	-
4	SCCS	3	1/2	6/64	1/3
5	SCCS-CWC	3	1/2	8/64	1/4

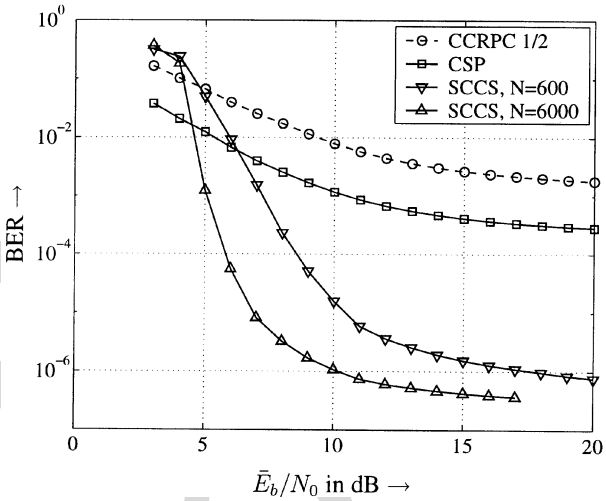

Fig. 9. Comparison of different coding schemes for $J = 32$ users, and $I = 10$ iterations for the SCCS.

both the stronger convolutional code with $R_{\rm CC} = 1/3$ and the stronger repetition code ($R_{\rm RPC} = 1/12$) yield an increased average minimum distance of the concatenated schemes.

C. Comparison of Coding Schemes

After optimizing the complex-valued SCCS-CWC, we have to compare it with the real-valued SCCS, with the conventional convolutional coding scheme and with the code-spread system. Therefore, we firstly consider real-valued coding schemes before comparing the SCCS-CWC with the SCCS. The parameters used in our investigations are given in Table III.

Fig. 8 shows the obtained results for $J = 1$ active user and $I = 10$ iterations. Reducing the code rate of the convolutional code from $R_{\rm CC} = 1/2$ down to $R_{\rm CC} = 1/8$ leads to an improvement of about 0.6 dB. A further reduction of $R_{\rm CC}$ leads asymptotically to the code-spread system and does not supply additional gains. Contrarily, the SCCS ($L_\Pi = 600$ and $L_\Pi = 6000$) achieves gains of 2–3 dB at a BER of 10^{-5}.

However, for low values of $\bar{E}_b/N_0$, the conventional convolutional coding schemes, as well as the code-spread system, are superior to the SCCS. Note that systems with high load are operating at very low SINRs. Thus, the question arises whether the SCCS is still superior to the other coding schemes if we increase the number of active users. Therefore, Fig. 9 shows results for $J = 32$ active users. In this case, the BER of the code-spread system does not achieve an error rate below $3 \cdot 10^{-4}$. Even for this extremely high load representing a fully loaded system, the SCCS reaches error rates down to 10^{-6}. At a BER of 10^{-5}, the larger interleaver leads to an additional gain of nearly 4 dB.

Besides considering the BER, we would like to emphasize that the computational decoding costs for the SCCS are lower than for the competing schemes because of the small constraint length of the outer convolutional code.

In a last step, we will include the complex-valued serial concatenation in our comparison (Table III). To do this, we confine our discussion on the scheme with an outer convolutional code of rate $R_{\rm CC} = 1/2$, an inner CWC of rate $R_{\rm CWC} = 8/64$, and a repetition code with $R_{\rm RPC} = 1/4$. This leads again to an overall code rate of $R = 1/64$ and allows a fair comparison between the coding schemes presented in this paper. The

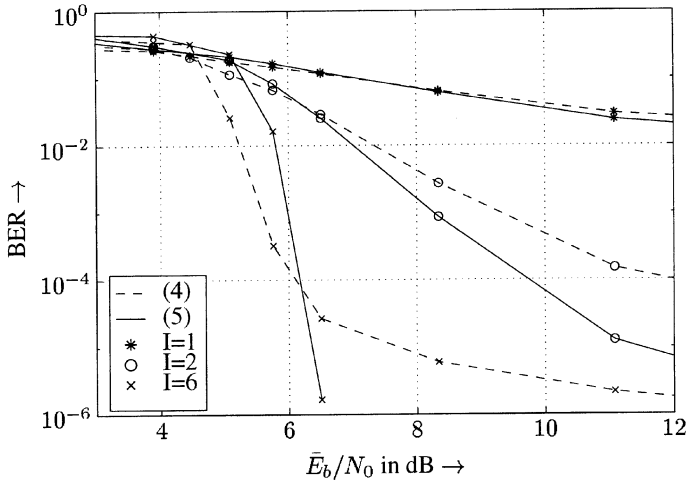

Fig. 10. Comparison of the SCCS (4) with rates $(1/2)/(6/64)/(1/3)$ and the SCCS-CWC (5) with rates $(1/2)/(8/64)/(1/4)$ for $J = 32$ users, $L_\Pi = 6000$, and $I = 1, 2, 6$ iterations.

SCCS consists of the same outer convolutional code as the complex-valued scheme, an inner WH code with $R_{\mathrm{WH}} = 6/64$, and a repetition code with $R_{\mathrm{RPC}} = 1/3$.

Fig. 10 presents Monte–Carlo simulation results in the case of a fully loaded system with $J = 32$ subscribers. The length of the interleaver is $L_\Pi = 6000$ for all systems, and the number of iterations equals $I = 1$, 2, and $I = 6$. We observe that the complex-valued scheme is superior for values of $\bar{E}_b/N_0$ larger than approximately 6 dB, while for small values, it performs marginally worse. Furthermore, it is quite remarkable that the proposed complex-valued scheme requires only about 6.3 dB to reach a BER of 10^{-6}. Note that we have a fully loaded CDMA system with $J = 32$ subscribers.

Concluding, we can state that the proposed complex as well as real-valued SCCSs with an inner WH code show remarkable error-correction capabilities even for fully loaded systems. Therefore, powerful low-rate coding is an appropriate mean for combating MAI.

V. Conclusion

This paper shows that significant performance improvements can be achieved by replacing the weak repetition code inherent in many CDMA systems by more powerful codes. Four different coding schemes have been examined; three of them are based on binary en-/decoding, i.e., the conventional scheme, the code-spread system, and a SCCS employing WH codes. The fourth coding scheme consists of an inner complex-valued block code. This code is based on a WH code that is extended by a QPSK modulation. Analytical derivation confirmed by simulation results shows a significantly better performance in comparison with (binary) WH codes.

Applying a complex-valued code as an inner code in a serial concatenation with an outer convolutional code, it turns out that convolutional codes with small constraint length perform best. Furthermore, strong inner coding with the complex-valued code and the repetition code is advantageous.

A detailed comparison of all four coding schemes shows that the serially concatenated systems (SCCS as well as SCCS-CWC) outperform the others significantly, especially for very high system load. Even in the case of a fully loaded system, BERs of 10^{-6} can be achieved, whereas the other two coding schemes suffer from an error floor at 10^{-4}. Note that the computational decoding costs of the SCCS are slightly lower than for the other three coding schemes.

Generally, we can state that powerful low-rate coding with serial concatenation including WH codes is suited to overcome the MAI when no multiuser detection is applied and multiple-user interference is interpreted as AWGN.

References

[1] E. Dahlman, B. Gudmundson, M. Nilsson, and J. Sköld, "UMTS/IMT-2000 based on wideband CDMA," *IEEE Commun. Mag.*, pp. 70–80, Sept. 1998.

[2] T. Ojanperä and R. Prasad, "Overview of air-interface multiple access for IMT-2000/UMTS," *IEEE Commun. Mag.*, pp. 82–95, Sept. 1998.

[3] A. Toskala, J. Castro, E. Dahlman, M. Latva-Aho, and T. Ojanperä, "Frames FMA2 wideband-CDMA for UMTS," *Eur. Trans. Commun.*, vol. 9, no. 4, pp. 325–335, Aug. 1998.

[4] "Requirements for the UMTS Terrestrial Radio Access System Special Mobile Group (SMG) (UMTS 04-01) (UTRA)," Eur. Telecommun. Standards Inst. (ETSI) Tech. Rep. Draft DTR/ETR (04-01), May 1997.

[5] S. Kaiser, "Multicarrier CDMA mobile radio systems—analysis and optimization of detection, decoding and channel estimation," Ph.D. dissertation, German Aerosp. Center VDI, Jan. 1998.

[6] A. Dekorsy and K. D. Kammeyer, "M-ary orthogonal modulation for MC-CDMA systems in indoor wireless radio networks," in *Proc. 1st Int. Workshop on MC-SS*, vol. 1, K. Fazel and G. P. Fettweis, Eds., Oberpfaffenhofen, Germany, Apr. 1997, pp. 69–76.

[7] A. Dekorsy, S. Fischer, and K. D. Kammeyer, "Maximum-likelihood decoding of M-ary orthogonal modulated signals for multicarrier spread-spectrum systems," in *Proc. IEEE Int. Symp. Personal, Indoor, Mobile Radio Communications (PIMRC)*, Boston, MA, Sept. 1998.

[8] A. Dekorsy and K. D. Kammeyer, "A new OFDM-CDMA uplink concept with M-ary orthogonal modulation," *Eur. Trans. Telecommun.*, vol. 10, no. 4, pp. 377–390, 1999.

[9] A. J. Viterbi, *CDMA—Principles of Spread Spectrum Communication*. Reading, MA: Addison-Wesley, 1995.

[10] ——, "Very low-rate convolutional codes for maximum theoretical performance of spread-spectrum multiple-access channels," *IEEE J. Select. Areas Commun.*, vol. 8, pp. 641–649, May 1990.

[11] P. Frenger, P. Orten, and T. Ottosson, "Code-spread CDMA using low-rate convolutional codes," in *Proc. IEEE Int. Symp. Spread Spectrum Techniques and Applications*, Sun City, South Africa, Sept. 1998, pp. 374–378.

[12] R. Herzog, A. Schmidbauer, and J. Hagenauer, "Iterative decoding and despreading improves CDMA-systems using M-ary orthogonal modulation and FEC," in *Proc. IEEE Int. Conf. Communications (ICC)*, vol. 2, Montreal, QC, Canada, June 8–12, 1997, pp. 909–913.

[13] V. Kühn, A. Dekorsy, and K. D. Kammeyer, "Channel coding aspects in an OFDM-CDMA system," in *Proc. 3rd ITG Conf. Source and Channel Coding*, Munich, Germany, Jan. 17–19, 2000, pp. 31–36.

[14] ——, "Low-rate channel coding for CDMA systems," *Int. J. Electron. Commun. (AEÜ)*, vol. 54, no. 6, pp. 353–363, Oct. 2000.

[15] K. D. Kammeyer and D. Nikolai, "A new CDMA concept using hybrid modulation with noncoherent detection," in *Proc. IEEE Fourth Symp. Communications and Vehicular Technology in the Benelux (SCVT'96)*, Gent, Belgium, Oct. 7–8, 1996, pp. 102–107.

[16] A. Dekorsy and K. D. Kammeyer, "Serial code concatenation with complex-valued Walsh–Hadamard codes applied to OFDM-CDMA," in *Proc. 3rd Int. Workshop on Multicarrier Spread Spectrum*, K. Fazel and S. Kaiser, Eds., Oberpfaffenhofen, Germany, Sept. 16–17, 2001.

[17] C. L. Weber, G. K. Huth, and B. H. Batson, "Performance considerations of code-division multiple-access systems," *IEEE Trans. Veh. Technol.*, vol. VT-30, no. 1, pp. 3–10, Feb. 1981.

[18] A. Dekorsy and K. D. Kammeyer, "Complex-valued block codes for OFDM-CDMA application," in *Proc. 2nd Int. Workshop on Multicarrier Spread Spectrum*, K. Fazel and S. Kaiser, Eds., Oberpfaffenhofen, Germany, Sept. 15–17, 1999, pp. 117–124.

[19] M. Bossert, *Kanalcodierung*, 2nd ed, B. G. Teubner, Ed. Stuttgart, Germany: Stuttgart, 1998.

[20] D. Nikolai, "Optimierung höherstufiger Codemultiplex-Systeme zur Mobilfunkübertragung," Ph.D. dissertation (in German), Forschungsberichte aus dem Arbeitsbereich Nachrichtentechnik der Universität Bremen, Bremen, Germany, Mar. 1998.
[21] A. Dekorsy, "Kanalcodierungskonzepte für Mehrträger-Codemultiplex in Mobilfunksystemen," Ph.D. dissertation (in German), Forschungsberichte aus dem Arbeitsbereich Nachrichtentechnik der Universität Bremen, Bremen, Germany, Jan. 2001.
[22] J. Hagenauer, E. Offer, and L. Papke, "Iterative decoding of binary block and convolutional codes," *IEEE Trans. Inform. Theory*, vol. 42, pp. 429–445, Mar. 1996.
[23] S. Benedetto, D. Divsalar, G. Montorsi, and F. Pollara, "Serial concatenation of interleaved codes: performance analysis, design, and iterative decoding," *IEEE Trans. Inform. Theory*, vol. 44, pp. 909–926, May 1998.
[24] P. Frenger, P. Orten, T. Ottosson, and A. Svensson, "Multirate convolutional codes,", Göteborg, Sweden, Tech. Rep. 21, Mar. 1998.
[25] S. Benedetto, G. Montorsi, D. Divsalar, and F. Pollara, "Serial concatenation of interleaved codes: performance analysis, design, and iterative decoding,", TDA Prog. Rep. 42–126, Aug. 1996.
[26] A. Dekorsy, V. Kühn, and K. D. Kammeyer, "Iterative decoding with M-ary orthogonal Walsh modulation in OFDM-CDMA," in *Proc. 1st Int. OFDM Workshop*, Hamburg-Harburg, Germany, Sept. 1999, pp. 23/1–23/5.

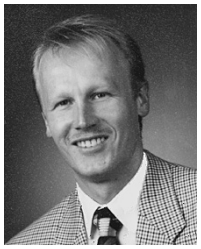

Armin Dekorsy (S'98–A'00) was born in Rielasingen, Germany, in 1967. He received the Dipl.-Ing. (FH) (B.Sc.) degree from Fachhochschule Konstanz, Germany, in 1992, the Dipl.-Ing. (M.Sc.) degree from the University of Paderborn, Paderborn, Germany, in 1995, and the Ph.D. degree from the University of Bremen, Bremen, Germany, in 2000, all in electrical engineering.

From September 2000 to February 2001, he was with T-Nova Deutsche Telekom Innovationsgesellschaft mbH, Technologiezentrum Darmstadt, Germany. In 2001 he joined Lucent Technologies Network Systems GmbH, Nuremberg, Germany, where he conducts research projects on UMTS. His current research interests are mainly smart antenna solutions and interference cancellation techniques, as well as radio resource management algorithms for third-generation mobile standards.

Volker Kuehn (M'00) was born in Paderborn, Germany, in 1966. He received the M.Sc. degree in electrical and electronics engineering from the University of Paderborn, Paderborn, Germany, in 1993, and the Ph.D. degree in communications engineering in 1998 from the same university.

Currently, he is with the Department of Communications Engineering at the University of Bremen, Bremen, Germany. His main fields of interest are error-correcting codes and iterative decoding, as well as CDMA.

Karl-Dirk Kammeyer (M'95) received the M.Sc. degree in electrical engineering from Berlin University of Technology, Berlin, Germany, in 1972, and the Ph.D. degree from Erlangen University, Erlangen, Germany, in 1977.

From 1972 to 1979, he worked in the field of data transmission, digital signal processing, and digital filters at the Universities of Berlin, Saarbrücken, and Erlangen, all in Germany. From 1979 to 1984, he was with Paderborn University, Paderborn, Germany, where he was engaged in the development of digital broadcasting systems. During the following decade, he was Professor for Digital Signal Processing in Communications at Hamburg University of Technology, Hamburg, Germany. In 1995, he was appointed Professor for Telecommunications at the University of Bremen, Bremen, Germany. His research interests are digital (adaptive) systems and signal processing in mobile communication systems (GSM, UMTS, multicarrier systems). Since 1989, he has been active in the field of higher order statistics. He holds 14 patent families, and has published two course books as well as 75 technical papers.